An Analytical Approach in Calculation of Noise Spectrum in Microwave Oscillators Based on Harmonic Balance

Esfandiar Mehrshahi and Forouhar Farzaneh, *Senior Member, IEEE*

***Abstract*—In this paper, a novel method for nonlinear analysis of noise in microwave oscillators is presented. Based on harmonic balance, the method is general from the point-of-view of circuit topology, noise sources spectral distribution, and their cross correlation. In this method, the effects such as frequency conversion and frequency modulation are considered simultaneously in a unified treatment. Relatively precise estimations for the output signal spectral density of an oscillator is practically obtained.**

***Index Terms*—Harmonic analysis, microwave oscillators, nonlinear circuits, oscillator noise, phase noise.**

I. Introduction

SPECTRAL purity of the microwave oscillators is of prime importance in microwave communication systems and radars so that its computation has become one of the concerns of microwave circuit designers. Many calculation methods in this regard are based on empirical relations and have taken into account only $1/f$ noise [1]–[3]. Using the pushing figure for computation of oscillator's $1/f$ noise spectrum is also an approximate method, which is simple and interesting [4]. Kurokawa has developed closed-form relations for a one-port oscillator's spectrum in the presence of uncorrelated noise sources [5]. Noise spectral analysis by conversion matrices is another method, which takes into account cross correlation of the noise sources, but is not accurate near the carrier due to frequency modulation effect [6]–[8]. Recently, a method has been devised that takes into account both conversion and modulation effects separately for far from carrier and near to the carrier [9]. The time-domain method has also been used, which by direct resolution of Longevin equations, computes the noise spectrum whether due to modulation or conversion [10], but it is time consuming.

In this paper, a unified treatment is presented which, based on the harmonic-balance resolution of a nonlinear multiport oscillator, computes directly the output spectrum at any port of the oscillator. The noise sources can be white or colored, and their cross correlation is taken into account in a matrix form. This method is completely analytical once the amplitude and frequency derivatives of the harmonic-balance characteristic equation are known.

In this paper, analytical results will be presented for the sake of comparison with existing references, the method is then applied to an MESFET oscillator, and the results are compared to the measurements of Anzill *et al.* [10].

Manuscript received March 9, 1999.

E. Mehrshahi is with the Shahid Beheshti University, Tehran, Iran.

F. Farzaneh is with the Department of Electrical Engineering, Sharif University of Technology, Tehran, Iran.

Publisher Item Identifier S 0018-9480(00)03750-9.

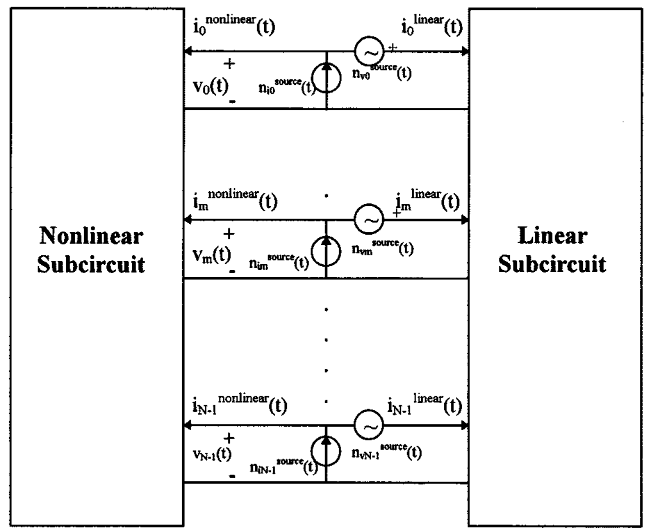

Fig. 1. General form of the oscillator circuit for harmonic-balance analysis.

II. Microwave-Oscillator Analysis by Harmonic Balance

The harmonic-balance method is a mixed frequency-time domain method for obtaining the steady-state periodic response of a nonlinear circuit [11], [12]. In this method, the circuit is divided into linear and nonlinear subcircuits, as in Fig. 1. All independent sources are transferred to the interconnecting ports. The noise sources are also referred to the interconnecting ports and represented by shunt current sources and series voltage sources. The unknowns are voltage vectors at all ports and harmonics. The linear subcircuit is analyzed in the frequency domain and the nonlinear subcircuit in the time domain.

A general form of the interconnecting port voltages can be represented as in

$$v_m(t) = \mathrm{Re}\sum_{k=0}^{H-1} V_{m,k}e^{jk\omega_0 t} = \mathrm{Re}\sum_{k=0}^{H-1} |V_{m,k}|e^{j(k\omega_0 t+\varphi_{0m,k})} \tag{1}$$

where $V_{m,k}$ and $\varphi_{0m,k}$ are their respective amplitude and phases. Writing the KCL at the interconnecting nodes, the harmonic-balance equation is obtained as follows:

$$\mathbf{F}(\mathbf{V},\omega_0) = \mathbf{I}(\mathbf{V}) + j\mathbf{\Omega}\mathbf{Q}(\mathbf{V}) + \mathbf{Y}(\omega_0)(\mathbf{V}+\mathbf{V}_{\text{source}}) - \mathbf{I}_{\text{source}} = 0. \tag{2}$$

In (2), the nonlinear subcircuit contains nonlinear transconductances and nonlinear transcapacitances. The resolution of this equation gives the voltage vectors at all ports and harmonics [11], [12].

III. Noise Sources Transfer to the Interconnecting Ports

In general, noise sources are dispersed in the network. In the nonlinear subcircuit, the intersecting nodes are chosen to be the noise sources ports; in the linear subcircuit, by linear transfer functions noise sources can be referred to the interconnecting ports. In the linear subcircuit, consider the noise sources vector as $\mathbf{n}_{\rm SL}(\omega)$. The members of this vector are functions of frequency. The nature of these sources can be described by the correlation matrix as in

$$\mathbf{C}_{\rm SL}(\omega) = \mathbf{n}_{\rm SL}(\omega)\mathbf{n}_{\rm SL}^{T*}(\omega) \tag{3}$$

where T^* signifies the transpose conjugate.

For transferring these sources to the connecting nodes, a transfer matrix can be defined such that

$$\mathbf{n}_{\rm SI}(\omega) = \mathbf{T}(\omega)\mathbf{n}_{\rm SL}(\omega). \tag{4}$$

By this transfer matrix, the Norton equivalent of the noise sources are determined at the interconnecting ports. The new correlation matrix would then be

$$\begin{aligned}\mathbf{C}_{\rm SI}(\omega) &= \mathbf{n}_{\rm SI}(\omega)\mathbf{n}_{\rm SI}^{T*}(\omega)\\ &= \mathbf{T}(\omega)\mathbf{n}_{\rm SL}(\omega)\mathbf{n}_{\rm SL}^{T*}(\omega)\mathbf{T}^{T*}(\omega)\\ &= \mathbf{T}(\omega)\mathbf{C}_{\rm SL}(\omega)\mathbf{T}^{T*}(\omega).\end{aligned} \tag{5}$$

Now taking into account the fact that linear subcircuit noise sources are uncorrelated with the nonlinear subcircuit noise sources, the correlation matrix of the total sources would be in form of

$$\mathbf{C}(\omega) = \mathbf{C}_{\rm SI}(\omega) + \mathbf{C}_{\rm SN}(\omega) \tag{6}$$

where $\mathbf{C}_{\rm SI}(\omega)$ signifies the correlation matrix of the linear subcircuit transferred to the interconnecting nodes, and $\mathbf{C}_{\rm SN}(\omega)$ signifies the correlation matrix of the nonlinear ports noise sources.

The noise-source currents at the interconnecting ports can be represented in a bandpass form about each harmonic, as in

$$n_m(t) = \mathrm{Re}\sum_{k=0}^{H-1} n_{m,k}(t)e^{jk\omega_0 t}. \tag{7}$$

As such, the general form of noise sources can be considered with regard to the spectral distribution, circuit topology, and their cross correlation.

IV. Noise Analysis, Amplitude, and Phase Fluctuations

In this section, we assume that the harmonic-balance analysis of the oscillator circuit has been performed and the steady-state values for harmonic voltages has been obtained [11]. From there on, the amplitude and phase fluctuations (modulations due to noise) are calculated, and from there after, the oscillator signal spectral density is derived. By presence of noise, the voltage vector members in (1) will be transformed into

$$v_m(t) = \mathrm{Re}\sum_{k=0}^{H-1}\Big(|V_{m,k}| + \Delta v_{m,k}(t)\Big)e^{j(k\omega_0 t + \varphi_{0m,k} + \varphi_{m,k}(t))} \tag{8}$$

where $\Delta v_{m,k}(t)$ represents amplitude fluctuations and $\varphi_{m,k}(t)$ represents the phase fluctuations due to noise. By the fact that noise sources are small compared to the harmonic voltages, we can assume that $|\Delta v_{m,k}(t)| \ll |V_{m,k}|$ and $(d\varphi_{m,k}(t)/dt) \ll \omega_0$. From there, (8) can be rewritten as

$$v_m(t) \approx \mathrm{Re}\sum_{k=0}^{H-1}\Big(|V_{m,k}| + \Delta v_{m,k}(t)\Big) \times e^{j\left(\left(k\omega_0 + \frac{d\varphi_{m,k}(t)}{dt} - \frac{j}{|V_{m,k}|}\frac{d\Delta v_{m,k}(t)}{dt}\right)t + \varphi_{0m,k}\right)} \tag{9}$$

where $k\omega_0 + (d\varphi_{m,k}(t)/dt) - (j/|V_{m,k}|)(d\Delta v_{m,k}(t)/dt)$ is the complex frequency. Inserting (9) in the harmonic-balance characteristic equation (2), putting noise components in the right-hand side, and expanding with the first-order derivatives, we obtain

$$\frac{\partial \mathbf{F}}{\partial|\mathbf{V}|}\Delta\mathbf{v}(t) + \left.\frac{\partial \mathbf{F}}{\partial\omega}\right|_{\omega=\omega_0}\left(\frac{d\varphi(t)}{dt} - j\frac{1}{|\mathbf{V}|}\frac{d\Delta\mathbf{v}(t)}{dt}\right) = \mathbf{n}(t). \tag{10}$$

Here, $(d\varphi(t)/dt) - j(1/|\mathbf{V}|)(d\Delta\mathbf{v}(t)/dt)$ is the offset complex frequency vector whose elements are $(d\varphi_{m,k}(t)/dt) - (j/|V_{m,k}|)(d\Delta v_{m,k}(t)/dt)$. Complex matrices $(\partial\mathbf{F}/\partial|\mathbf{V}|)$ and $(\partial\mathbf{F}/\partial\omega)$ are the amplitude and frequency derivatives of the vector $\mathbf{F}$. Separating real and imaginary parts of (10), one obtains a system of matrix equations, shown in (11) and (12), at the bottom of this page. Now, by transforming (11) into the

$$\begin{cases}\dfrac{\partial \mathbf{F}^{\mathbf{r}}}{\partial|\mathbf{V}|}\Delta\mathbf{v}(t) + \left.\dfrac{\partial \mathbf{F}^{\mathbf{r}}}{\partial\omega}\right|_{\omega=\omega_0}\dfrac{d\varphi(t)}{dt} + \left.\dfrac{\partial \mathbf{F}^{\mathbf{i}}}{\partial\omega}\right|_{\omega=\omega_0}\dfrac{1}{|\mathbf{V}|}\dfrac{d\Delta\mathbf{v}(t)}{dt} = \mathbf{n}^{\mathbf{r}}(t)\\ \dfrac{\partial \mathbf{F}^{\mathbf{i}}}{\partial|\mathbf{V}|}\Delta\mathbf{v}(t) + \left.\dfrac{\partial \mathbf{F}^{\mathbf{i}}}{\partial\omega}\right|_{\omega=\omega_0}\dfrac{d\varphi(t)}{dt} - \left.\dfrac{\partial \mathbf{F}^{\mathbf{r}}}{\partial\omega}\right|_{\omega=\omega_0}\dfrac{1}{|\mathbf{V}|}\dfrac{d\Delta\mathbf{v}(t)}{dt} = \mathbf{n}^{\mathbf{i}}(t)\end{cases} \tag{11}$$

$$\begin{cases}\dfrac{\partial \mathbf{F}^{\mathbf{r}}}{\partial|\mathbf{V}|}\Delta\mathbf{v}(\omega) + \left.\dfrac{\partial \mathbf{F}^{\mathbf{r}}}{\partial\omega}\right|_{\omega=\omega_0}j\omega\varphi(\omega) + \left.\dfrac{\partial \mathbf{F}^{\mathbf{i}}}{\partial\omega}\right|_{\omega=\omega_0}\dfrac{j\omega}{|\mathbf{V}|}\Delta\mathbf{v}(\omega) = \mathbf{n}^{\mathbf{r}}(\omega)\\ \dfrac{\partial \mathbf{F}^{\mathbf{i}}}{\partial|\mathbf{V}|}\Delta\mathbf{v}(\omega) + \left.\dfrac{\partial \mathbf{F}^{\mathbf{i}}}{\partial\omega}\right|_{\omega=\omega_0}j\omega\varphi(\omega) - \left.\dfrac{\partial \mathbf{F}^{\mathbf{r}}}{\partial\omega}\right|_{\omega=\omega_0}\dfrac{j\omega}{|\mathbf{V}|}\Delta\mathbf{v}(\omega) = \mathbf{n}^{\mathbf{i}}(\omega)\end{cases} \tag{12}$$

$$\mathbf{A}_1 = \begin{bmatrix} \left.\frac{\partial F_{0,0}}{\partial \omega}\right|_{\omega=\omega_0} \left.\frac{\partial F_{0,0}}{\partial \omega}\right|^*_{\omega=\omega_0} \frac{1}{|V_{0,0}|} & 0 & \cdots & 0 & \cdots & 0 \\ 0 & \left.\frac{\partial F_{0,1}}{\partial \omega}\right|_{\omega=\omega_0} \left.\frac{\partial F_{0,1}}{\partial \omega}\right|^*_{\omega=\omega_0} \frac{1}{|V_{0,1}|} & \cdots & 0 & \cdots & 0 \\ \vdots & \vdots & \ddots & & & \vdots \\ 0 & 0 & & \left.\frac{\partial F_{m,k}}{\partial \omega}\right|_{\omega=\omega_0} \left.\frac{\partial F_{m,k}}{\partial \omega}\right|^*_{\omega=\omega_0} \frac{1}{|V_{m,k}|} & & 0 \\ \vdots & \vdots & & & \ddots & \vdots \\ 0 & 0 & \cdots & 0 & \cdots & \left.\frac{\partial F_{N-1,H-1}}{\partial \omega}\right|_{\omega=\omega_0} \left.\frac{\partial F_{N-1,H-1}}{\partial \omega}\right|^*_{\omega=\omega_0} \frac{1}{|V_{N-1,H-1}|} \end{bmatrix} \tag{15}$$

$$\mathbf{A}_2 = \begin{bmatrix} \left.\frac{\partial F^{\mathbf{r}}_{0,0}}{\partial \omega}\right|_{\omega=\omega_0} \frac{j\omega}{|V_{0,0}|} & 0 & \cdots & 0 & \cdots & 0 \\ 0 & \left.\frac{\partial F^{\mathbf{r}}_{0,1}}{\partial \omega}\right|_{\omega=\omega_0} \frac{j\omega}{|V_{0,1}|} & \cdots & 0 & \cdots & 0 \\ \vdots & \vdots & \ddots & & & \vdots \\ 0 & 0 & & \left.\frac{\partial F^{\mathbf{r}}_{m,k}}{\partial \omega}\right|_{\omega=\omega_0} \frac{j\omega}{|V_{m,k}|} & & 0 \\ \vdots & \vdots & & & \ddots & \vdots \\ 0 & 0 & \cdots & 0 & \cdots & \left.\frac{\partial F^{\mathbf{r}}_{N-1,H-1}}{\partial \omega}\right|_{\omega=\omega_0} \frac{j\omega}{|V_{N-1,H-1}|} \end{bmatrix} \tag{16}$$

$$\mathbf{A}_3 = \begin{bmatrix} \left.\frac{\partial F^{\mathbf{i}}_{0,0}}{\partial \omega}\right|_{\omega=\omega_0} \frac{j\omega}{|V_{0,0}|} & 0 & \cdots & 0 & \cdots & 0 \\ 0 & \left.\frac{\partial F^{\mathbf{i}}_{0,1}}{\partial \omega}\right|_{\omega=\omega_0} \frac{j\omega}{|V_{0,1}|} & \cdots & 0 & \cdots & 0 \\ \vdots & \vdots & \ddots & & & \vdots \\ 0 & 0 & & \left.\frac{\partial F^{\mathbf{i}}_{m,k}}{\partial \omega}\right|_{\omega=\omega_0} \frac{j\omega}{|V_{m,k}|} & & 0 \\ \vdots & \vdots & & & \ddots & \vdots \\ 0 & 0 & \cdots & 0 & \cdots & \left.\frac{\partial F^{\mathbf{i}}_{N-1,H-1}}{\partial \omega}\right|_{\omega=\omega_0} \frac{j\omega}{|V_{N-1,H-1}|} \end{bmatrix} \tag{17}$$

frequency domain, one obtains (12). The resolution of this set of equations gives $\Delta\mathbf{v}(\omega)$ and $\varphi(\omega)$ vectors as follows:

$$\Delta V(\omega) = \left[\left(\frac{\partial\mathbf{F^r}}{\partial|\mathbf{V}|}\frac{\partial\mathbf{F^i}}{\partial\omega}\bigg|_{\omega=\omega_0} - \frac{\partial\mathbf{F^i}}{\partial|\mathbf{V}|}\frac{\partial\mathbf{F^r}}{\partial\omega}\bigg|_{\omega=\omega_0}\right) + j\omega\mathbf{A}_1\right]^{-1} \times \left[\frac{\partial\mathbf{F^i}}{\partial\omega}\bigg|_{\omega=\omega_0}\mathbf{n^r}(\omega) - \frac{\partial\mathbf{F^r}}{\partial\omega}\bigg|_{\omega=\omega_0}\mathbf{n^i}(\omega)\right] \tag{13}$$

$$\Phi(\omega) = \frac{1}{j\omega}\left[\left(\frac{\partial\mathbf{F^i}}{\partial|\mathbf{V}|}\frac{\partial\mathbf{F^r}}{\partial\omega}\bigg|_{\omega=\omega_0} - \frac{\partial\mathbf{F^r}}{\partial|\mathbf{V}|}\frac{\partial\mathbf{F^i}}{\partial\omega}\bigg|_{\omega=\omega_0}\right) - j\omega\mathbf{A}_1\right]^{-1} \times \left[\left(\frac{\partial\mathbf{F^i}}{\partial|\mathbf{V}|} - \mathbf{A}_2\right)\mathbf{n^r}(\omega) - \left(\frac{\partial\mathbf{F^r}}{\partial|\mathbf{V}|} + \mathbf{A}_3\right)\mathbf{n^i}(\omega)\right] \tag{14}$$

where $\mathbf{A}_1$, $\mathbf{A}_2$ and $\mathbf{A}_3$ are coefficient matrices defined by (15)–(17), shown on the previous page.

V. Signals Spectra at the Interconnecting Ports

Having calculated $\Delta\mathbf{v}(\omega)$ and $\varphi(\omega)$ in the previous section, we are in a position to calculate the oscillator's signal spectrum at any interconnecting ports. For this purpose, we first introduce the correlation matrix of the voltages at ports and harmonics by (18), shown at the bottom of this page. The elements of (18) are the cross correlation between different port voltages at different harmonics, defined by

$$R_{v_{m,k},v_{n,l}}(\tau) = \lim_{T\to\infty}\frac{1}{T}\int_{-\frac{T}{2}}^{\frac{T}{2}} v_{m,k}(t)v_{n,1}(t+\tau)\,dt. \tag{19}$$

$$\mathbf{R}_v(\tau) = \begin{bmatrix} R_{v_{0,0},v_{0,0}}(\tau) & R_{v_{0,0},v_{0,1}}(\tau) & \cdots & R_{v_{0,0},v_{m,k}}(\tau) & \cdots & R_{v_{0,0},v_{N-1,H-1}}(\tau) \\ R_{v_{0,1},v_{0,0}}(\tau) & R_{v_{0,1},v_{0,1}}(\tau) & \cdots & R_{v_{0,1},v_{m,k}}(\tau) & \cdots & R_{v_{0,1},v_{N-1,H-1}}(\tau) \\ \vdots & \vdots & & \vdots & & \vdots \\ R_{v_{m,k},v_{0,0}}(\tau) & R_{v_{m,k},v_{0,1}}(\tau) & \cdots & R_{v_{m,k},v_{m,k}}(\tau) & \cdots & R_{v_{m,k},v_{N-1,H-1}}(\tau) \\ \vdots & \vdots & & \vdots & & \vdots \\ R_{v_{N-1,H-1},v_{0,0}}(\tau) & R_{v_{N-1,H-1},v_{0,1}}(\tau) & \cdots & R_{v_{N-1,H-1},v_{m,k}}(\tau) & \cdots & R_{v_{N-1,H-1},v_{N-1,H-1}}(\tau) \end{bmatrix} \tag{18}$$

$$\begin{aligned} G_{v_{m,k},v_{n,k}}(\omega) &= \frac{|V_{m,k}||V_{n,k}|}{4} \\ &\times \Bigg\{ \cos(\varphi_{0m,k} - \varphi_{0n,k}) \Bigg[\left(1 - \frac{1}{4\pi}\int_{-\infty}^{\infty}\Big(\Phi_{m,k}(\omega)\Big)\Big(\Phi_{m,k}(\omega)\Big)^* d\omega - \frac{1}{4\pi}\int_{-\infty}^{\infty}\Big(\Phi_{n,k}(\omega)\Big)\Big(\Phi_{n,k}(\omega)\Big)^* d\omega\right)\delta(\Omega_k) \\ &\quad + \frac{\Big(\Delta V_{m,k}(\Omega_k)\Big)\Big(\Delta V_{n,k}(\Omega_k)\Big)^*}{|V_{m,k}||V_{n,k}|} + \Big(\Phi_{m,k}(\Omega_k)\Big)\Big(\Phi_{n,k}(\Omega_k)\Big)^* \\ &\quad - j\Bigg[\frac{\Big(\Phi_{m,k}(\Omega_k)\Big)\Big(\Delta V_{n,k}(\Omega_k)\Big)^*}{|V_{n,k}|} - \frac{\Big(\Phi_{n,k}(\Omega_k)\Big)^*\Big(\Delta V_{m,k}(\Omega_k)\Big)}{|V_{m,k}|} \\ &\quad + \frac{\delta(\Omega_k)}{2\pi}\left[\int_{-\infty}^{\infty}\frac{\Big(\Delta V_{m,k}(\omega)\Big)}{|V_{m,k}|}\Big(\Phi_{m,k}(\omega)\Big)^* d\omega - \int_{-\infty}^{\infty}\frac{\Big(\Delta V_{m,k}(\omega)\Big)}{|V_{m,k}|}\Big(\Phi_{n,k}(\omega)\Big)^* d\omega\right]\Bigg]\Bigg] \\ &\quad + \sin(\varphi_{0m,k} - \varphi_{0n,k}) \Bigg[-\Bigg[\frac{\Big(\Phi_{m,k}(\Omega_k)\Big)\Big(\Delta V_{n,k}(\Omega_k)\Big)^*}{|V_{n,k}|} - \frac{\Big(\Phi_{n,k}(\Omega_k)\Big)^*\Big(\Delta V_{m,k}(\Omega_k)\Big)}{|V_{m,k}|} \\ &\quad + \frac{\delta(\Omega_k)}{2\pi}\left[\int_{-\infty}^{\infty}\frac{\Big(\Delta V_{m,k}(\omega)\Big)}{|V_{m,k}|}\Big(\Phi_{m,k}(\omega)\Big)^* d\omega - \int_{-\infty}^{\infty}\frac{\Big(\Delta V_{m,k}(\omega)\Big)}{|V_{m,k}|}\Big(\Phi_{n,k}(\omega)\Big)^* d\omega\right]\Bigg] \\ &\quad - j\Bigg[\left(1 - \frac{1}{4\pi}\int_{-\infty}^{\infty}\Big(\Phi_{m,k}(\omega)\Big)\Big(\Phi_{m,k}(\omega)\Big)^* d\omega - \frac{1}{4\pi}\int_{-\infty}^{\infty}\Big(\Phi_{n,k}(\omega)\Big)\Big(\Phi_{n,k}(\omega)\Big)^* d\omega\right)\delta(\Omega_k) \\ &\quad + \frac{\Big(\Delta V_{m,k}(\Omega_k)\Big)\Big(\Delta V_{n,k}(\Omega_k)\Big)^*}{|V_{m,k}||V_{n,k}|} + \Big(\Phi_{m,k}(\Omega_k)\Big)\Big(\Phi_{n,k}(\Omega_k)\Big)\Bigg]\Bigg]\Bigg\} \end{aligned} \tag{21}$$

The calculation of integrals involved in (19) for $k=l$ results in (20) (see Appendix A). Note that $R_{v_{m,k},v_{n,1}}(\tau)=0$ for $k\neq l$.

$$\begin{aligned}
&R_{v_{m,k},v_{n,k}}(\tau)\\
&\quad=\frac{|V_{m,k}||V_{n,k}|}{2}\\
&\quad\cdot\Bigg[\cos(k\omega_0\tau-\varphi_{0m,k}+\varphi_{0n,k})\\
&\quad\times\Big[1-.5\left(R_{\varphi_{m,k},\varphi_{m,k}}(0)+R_{\varphi_{n,k},\varphi_{n,k}}(0)\right)\\
&\qquad+R_{\frac{\Delta v_{m,k}}{|V_{m,k}|},\frac{\Delta v_{n,k}}{|V_{n,k}|}}(\tau)+R_{\varphi_{m,k},\varphi_{n,k}}(\tau)\Big]\\
&\quad+\sin(k\omega_0\tau-\varphi_{0m,k}+\varphi_{0n,k})\\
&\quad\times\Big[R_{\varphi_{m,k},\frac{\Delta v_{n,k}}{|V_{n,k}|}}(\tau)-R_{\frac{\Delta v_{m,k}}{|V_{m,k}|},\varphi_{n,k}}(\tau)\\
&\qquad+R_{\frac{\Delta v_{m,k}}{|V_{m,k}|},\varphi_{m,k}}(0)-R_{\varphi_{n,k},\frac{\Delta v_{n,k}}{|V_{n,k}|}}(0)\Big]\Bigg]
\end{aligned}\tag{20}$$

where $R_{\varphi_{m,k},\varphi_{n,k}}(\tau)$ and $R_{(\Delta v_{m,k}/|V_{m,k}|),(\Delta v_{n,k}/|V_{n,k}|)}(\tau)$ are the phase and amplitude autocorrelation functions, respectively, and $R_{\varphi_{m,k},(\Delta v_{n,k}/|V_{n,k}|)}(\tau)$ is the phase–amplitude cross-correlation function. The Fourier transform of the correlation matrix $\mathbf{R}_v(\tau)$ results in $\mathbf{G}_v(\omega)$, the spectral density matrix; this is an involved matrix, whose elements are given by (21), shown at the bottom of the prevous page, where $\Omega_k=\omega-k\omega_0$ is the offset frequency from the kth harmonic. Off the diagonal elements give the cross-correlation spectrum; the diagonal elements of this matrix give the power spectral densities of the port m at the kth harmonic as in

$$\begin{aligned}
&G_{v_{m,k},v_{m,k}}(\omega)\\
&\quad=\frac{|V_{m,k}|^2}{4}\Bigg[\left(1-\frac{1}{2\pi}\int_{-\infty}^{\infty}\left(\Phi_{m,k}(\omega)\right)\left(\Phi_{m,k}(\omega)\right)^*d\omega\right)\\
&\qquad\times\delta(\Omega_k)+\frac{\left(\Delta V_{m,k}(\Omega_k)\right)\left(\Delta V_{m,k}(\Omega_k)\right)^*}{|V_{m,k}|^2}\\
&\qquad+\left(\Phi_{m,k}(\Omega_k)\right)\left(\Phi_{m,k}(\Omega_k)\right)^*\\
&\qquad+2\,\mathrm{Im}\,\frac{\left(\Phi_{m,k}(\Omega_k)\right)\left(\Delta V_{m,k}(\Omega_k)\right)^*}{|V_{m,k}|}\Bigg]
\end{aligned}\tag{22}$$

In this spectrum, one can separate amplitude and phase noise contributions as in (23), shown at the bottom of this page, and (24), shown at the bottom of this page. Here, the power spectral densities at ports and harmonics are expressed in terms of phase and amplitude fluctuations and cross-correlation spectral densities, given by (25)–(27), shown at the bottom of the following page. These quantities, in turn, can be readily reduced from (13) and (14). As such, we have obtained a complete set of analytical expressions for determining power spectral densities at the interconnecting ports of the oscillator, the only thing needed to compute these spectral densities, given the noise sources, is the matrix form derivatives of the harmonic-balance characteristics equation.

VI. Spectral Density at the Output Port

We now have known the spectral densities at the interconnecting ports. It is quite often needed to compute the spectral

$$G^{AM}_{v_{m,k},v_{n,k}}(\omega)=\begin{cases}\dfrac{|V_{m,k}||V_{n,k}|}{4}\left[\cos(\varphi_{0m,k}-\varphi_{0n,k})\left[\delta(\Omega_k)+\dfrac{\left(\Delta V_{m,k}(\Omega_k)\right)\left(\Delta V_{n,k}(\Omega_k)\right)^*}{|V_{m,k}||V_{n,k}|}\right]\right.\\ \left.-j\sin(\varphi_{0m,k}-\varphi_{0n,k})\left[\dfrac{\left(\Delta V_{m,k}(\Omega_k)\right)\left(\Delta V_{n,k}(\Omega_k)\right)^*}{|V_{m,k}||V_{n,k}|}\right]\right], & \text{for } m\neq n\\ \dfrac{|V_{m,k}|^2}{4}\left[\delta(\Omega_k)+\dfrac{\left(\Delta V_{m,k}(\Omega_k)\right)\left(\Delta V_{m,k}(\Omega_k)\right)^*}{|V_{m,k}|^2}\right], & \text{for } m=n\end{cases}\tag{23}$$

$$\begin{aligned}
&G^{PM}_{v_{m,k},v_{n,k}}(\omega)\\
&=\begin{cases}\dfrac{|V_{m,k}||V_{n,k}|}{4}\\
\times\Bigg[\cos(\varphi_{0m,k}-\varphi_{0n,k})\Bigg[\left(1-\dfrac{1}{4\pi}\displaystyle\int_{-\infty}^{\infty}\left(\Phi_{m,k}(\omega)\right)\left(\Phi_{m,k}(\omega)\right)^*d\omega-\dfrac{1}{4\pi}\displaystyle\int_{-\infty}^{\infty}\left(\Phi_{n,k}(\omega)\right)\left(\Phi_{n,k}(\omega)\right)^*d\omega\right)\delta(\Omega_k)\\
\quad+\left(\Phi_{m,k}(\Omega_k)\right)\left(\Phi_{n,k}(\Omega_k)\right)^*\Bigg]-j\sin(\varphi_{0m,k}-\varphi_{0n,k})\\
\times\Bigg[\left(1-\dfrac{1}{4\pi}\displaystyle\int_{-\infty}^{\infty}\left(\Phi_{m,k}(\omega)\right)\left(\Phi_{m,k}(\omega)\right)^*d\omega-\dfrac{1}{4\pi}\displaystyle\int_{-\infty}^{\infty}\left(\Phi_{n,k}(\omega)\right)\left(\Phi_{n,k}(\omega)\right)^*d\omega\right)\delta(\Omega_k)\\
\quad+\left(\Phi_{m,k}(\Omega_k)\right)\left(\Phi_{n,k}(\Omega_k)\right)\Bigg]\Bigg], \qquad \text{for } m\neq n\\
\dfrac{|V_{m,k}|^2}{4}\left[\left(1-\dfrac{1}{2\pi}\displaystyle\int_{-\infty}^{\infty}\left(\Phi_{m,k}(\omega)\right)\left(\Phi_{m,k}(\omega)\right)^*d\omega\right)\delta(\Omega_k)+\left(\Phi_{m,k}(\Omega_k)\right)\left(\Phi_{m,k}(\Omega_k)\right)^*\right], \qquad \text{for } m=n\end{cases}
\end{aligned}\tag{24}$$

density at a specified port connected to the linear subcircuit. For this purpose, consider the circuit connection shown in Fig. 2. It is possible to calculate the voltage at port "L" from the voltages at the interconnecting ports through a linear transformation.

In (28), T_L is a $H \times NH$ matrix, which performs this transformation.

$$\mathbf{V}_L = \begin{bmatrix} V_{L0} \\ V_{L1} \\ \vdots \\ V_{Lk} \\ \vdots \\ V_{L(H-1)} \end{bmatrix} = \mathbf{T}_L \mathbf{V}. \quad (28)$$

The spectral density vector at port "L" would then become

$$\mathbf{G}_L(\omega) = \mathbf{T}_L(\omega)\mathbf{G}_v(\omega)\mathbf{T}_L^{T*}(\omega). \quad (29)$$

Regarding (29), the total single-sideband noise of the oscillator at port "L" and frequency $f_m = f - kf_0$ normalized to the carrier level can be expressed as (30), shown at the bottom of the following page, where $\alpha = 1 - (1/2\pi)\int_{-\infty}^{\infty} (\Phi_{Lk}(\omega))(\Phi_{Lk}(\omega))^* \, d\omega$ is nearly equal to unity.

VII. Applications

A. Noise Spectrum in Kurokawa Oscillator

As an example, we consider a one-port oscillator. Fig. 3 shows a simple oscillator model used by Kurokawa [5], in

$$\begin{aligned}\Delta\mathbf{V}(\omega)\Delta\mathbf{V}(\omega)^{T*} =& \left[\left(\frac{\partial\mathbf{F^r}}{\partial|\mathbf{V}|}\frac{\partial\mathbf{F^i}}{\partial\omega}\bigg|_{\omega=\omega_0} - \frac{\partial\mathbf{F^i}}{\partial|\mathbf{V}|}\frac{\partial\mathbf{F^r}}{\partial\omega}\bigg|_{\omega=\omega_0}\right) + j\omega\mathbf{A}_1\right]^{-1} \\ &\times\left[\frac{\partial\mathbf{F^i}}{\partial\omega}\bigg|_{\omega=\omega_0}\mathbf{C^{rr}}(\omega)\,\frac{\partial\mathbf{F^i}^{T*}}{\partial\omega}\bigg|_{\omega=\omega_0} - \frac{\partial\mathbf{F^i}}{\partial\omega}\bigg|_{\omega=\omega_0}\mathbf{C^{ri}}(\omega)\,\frac{\partial\mathbf{F^r}^{T*}}{\partial\omega}\bigg|_{\omega=\omega_0}\frac{\partial\mathbf{F^r}}{\partial\omega}\bigg|_{\omega=\omega_0}\right. \\ &\left.\times\mathbf{C^{ir}}(\omega)\,\frac{\partial\mathbf{F^i}^{T*}}{\partial\omega}\bigg|_{\omega=\omega_0} - \frac{\partial\mathbf{F^r}}{\partial\omega}\bigg|_{\omega=\omega_0}\mathbf{C^{ii}}(\omega)\,\frac{\partial\mathbf{F^r}^{T*}}{\partial\omega}\bigg|_{\omega=\omega_0}\right] \\ &\times\left[\left(\frac{\partial\mathbf{F^r}}{\partial|\mathbf{V}|}\frac{\partial\mathbf{F^i}}{\partial\omega}\bigg|_{\omega=\omega_0} - \frac{\partial\mathbf{F^i}}{\partial|\mathbf{V}|}\frac{\partial\mathbf{F^r}}{\partial\omega}\bigg|_{\omega=\omega_0}\right) + j\omega\mathbf{A}_1\right]^{-T*} \quad (25)\end{aligned}$$

$$\begin{aligned}\Phi(\omega)\Phi(\omega)^{T*} =& \frac{1}{\omega^2}\left[\left(\frac{\partial\mathbf{F^i}}{\partial|\mathbf{V}|}\frac{\partial\mathbf{F^r}}{\partial\omega}\bigg|_{\omega=\omega_0} - \frac{\partial\mathbf{F^r}}{\partial|\mathbf{V}|}\frac{\partial\mathbf{F^i}}{\partial\omega}\bigg|_{\omega=\omega_0}\right) - j\omega\mathbf{A}_1\right]^{-1} \\ &\times\left[\left(\frac{\partial\mathbf{F^i}}{\partial|\mathbf{V}|} - \mathbf{A}_2\right)\mathbf{C^{rr}}(\omega)\left(\frac{\partial\mathbf{F^i}}{\partial|\mathbf{V}|} - \mathbf{A}_2\right)^{T*} - \left(\frac{\partial\mathbf{F^i}}{\partial|\mathbf{V}|} - \mathbf{A}_2\right)\mathbf{C^{ri}}(\omega)\left(\frac{\partial\mathbf{F^r}}{\partial\omega}\bigg|_{\omega=\omega_0} + \mathbf{A}_3\right)^{T*}\right. \\ &\left.- \left(\frac{\partial\mathbf{F^r}}{\partial\omega}\bigg|_{\omega=\omega_0} + \mathbf{A}_3\right)\mathbf{C^{ir}}(\omega)\left(\frac{\partial\mathbf{F^i}}{\partial|\mathbf{V}|} - \mathbf{A}_2\right)^{T*} + \left(\frac{\partial\mathbf{F^r}}{\partial\omega}\bigg|_{\omega=\omega_0} + \mathbf{A}_3\right)\mathbf{C^{ii}}(\omega)\times\left(\frac{\partial\mathbf{F^r}}{\partial\omega}\bigg|_{\omega=\omega_0} + \mathbf{A}_3\right)^{T*}\right] \\ &\times\left[\left(\frac{\partial\mathbf{F^i}}{\partial|\mathbf{V}|}\frac{\partial\mathbf{F^r}}{\partial\omega}\bigg|_{\omega=\omega_0} - \frac{\partial\mathbf{F^r}}{\partial|\mathbf{V}|}\frac{\partial\mathbf{F^i}}{\partial\omega}\bigg|_{\omega=\omega_0}\right) - j\omega\mathbf{A}_1\right]^{-T*} \quad (26)\end{aligned}$$

$$\begin{aligned}\Delta\mathbf{V}(\omega)\Phi(\omega)^{T*} =& \left[\left(\frac{\partial\mathbf{F^r}}{\partial|\mathbf{V}|}\frac{\partial\mathbf{F^i}}{\partial\omega}\bigg|_{\omega=\omega_0} - \frac{\partial\mathbf{F^i}}{\partial|\mathbf{V}|}\frac{\partial\mathbf{F^r}}{\partial\omega}\bigg|_{\omega=\omega_0}\right) + j\omega\mathbf{A}_1\right]^{-1} \\ &\times\left[\frac{\partial\mathbf{F^i}}{\partial\omega}\bigg|_{\omega=\omega_0}\mathbf{C^{rr}}(\omega)\left(\frac{\partial\mathbf{F^i}}{\partial|\mathbf{V}|} - \mathbf{A}_2\right)^{T^*} - \frac{\partial\mathbf{F^i}}{\partial\omega}\bigg|_{\omega=\omega_0}\mathbf{C^{ri}}(\omega)\left(\frac{\partial\mathbf{F^r}}{\partial\omega}\bigg|_{\omega=\omega_0} + \mathbf{A}_3\right)^{T^*}\frac{\partial\mathbf{F^r}}{\partial\omega}\bigg|_{\omega=\omega_0}\right. \\ &\left.\times\mathbf{C^{ir}}(\omega)\left(\frac{\partial\mathbf{F^i}}{\partial|V|} - \mathbf{A}_2\right)^{T^*} - \frac{\partial\mathbf{F^r}}{\partial\omega}\bigg|_{\omega=\omega_0}\mathbf{C^{ii}}(\omega)\left(\frac{\partial\mathbf{F^r}}{\partial\omega}\bigg|_{\omega=\omega_0} + \mathbf{A}_3\right)^{T^*}\right] \\ &\times\frac{j}{\omega}\left[\left(\frac{\partial\mathbf{F^i}}{\partial|\mathbf{V}|}\frac{\partial\mathbf{F^r}}{\partial\omega}\bigg|_{\omega=\omega_0} - \frac{\partial\mathbf{F^r}}{\partial|\mathbf{V}|}\frac{\partial\mathbf{F^i}}{\partial\omega}\bigg|_{\omega=\omega_0}\right) - j\omega\mathbf{A}_1\right]^{T^*} \quad (27)\end{aligned}$$

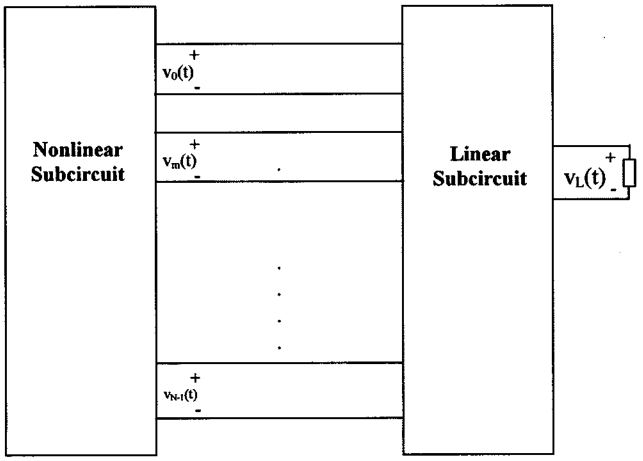

Fig. 2. Transformation of interconnecting voltages to port "L," through a linear subcircuit.

which the nonlinear elements are represented by its admittance describing function (first-order harmonic balance). $n_i(t)$ represents the only noise current source present in the circuit. The characteristics equation of the oscillator is given by

$$F(V,\omega_0) = \big(Y_L(\omega_0) + Y_{\rm NL}(V,\omega_0)\big)V = 0 \tag{31a}$$

$$Y_L(\omega_0) + Y_{\rm NL}(V,\omega_0) = Y_T(V,\omega_0) = G_T(V,\omega_0) + jB_T(V,\omega_0). \tag{31b}$$

By taking the noise current source into account and adding it to the right-hand side of (31a), Kurokawa has resolved these equations with the assumption of zero cross correlation between in-phase and quadrature noise components. In addition, he has considered that the two components of noise have equal spectral densities. Equation (32) describes the phase noise component obtained by Kurokawa [5] as follows:

$$\ell(f_m) = \frac{\eta}{V^2\omega_m^2} \times \frac{\left(\frac{\partial G_T}{\partial V}\right)^2 + \left(\frac{\partial B_T}{\partial V}\right)^2 + \frac{\omega_m^2}{V^2}\left(\left(\frac{\partial G_T}{\partial \omega}\right)^2 + \left(\frac{\partial B_T}{\partial \omega}\right)^2\right)}{\left(\frac{\partial G_T}{\partial \omega}\frac{\partial B_T}{\partial V} - \frac{\partial G_T}{\partial V}\frac{\partial B_T}{\partial \omega}\right)^2 + \frac{\omega_m^2}{V^2}\left(\left(\frac{\partial G_T}{\partial \omega}\right)^2 + \left(\frac{\partial B_T}{\partial \omega}\right)^2\right)^2}. \tag{32}$$

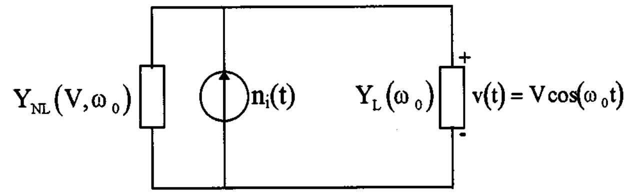

Fig. 3. Simplified one-port oscillator model.

Later, Rizzoli *et al.* [9] have taken into account the cross correlation between in-phase and quadrature noise components. The relations of (33) describe the correlation matrix elements

$$\begin{cases} n(t) = n_i(t) = {\rm Re}(n^c(t)e^{j\omega_0 t}) = n^r(t)\cos(\omega_0 t) + n^i(t)\sin(\omega_0 t) \\ \mathbf{C}^{rr}(\omega) = n^r(\omega)n^{r^*}(\omega) = \eta_1 \\ \mathbf{C}^{ri}(\omega) = n^r(\omega)n^{i^*}(\omega) = \eta_2 \\ \mathbf{C}^{ir}(\omega) = n^i(\omega)n^{r^*}(\omega) = \eta_2^* \\ \mathbf{C}^{ii}(\omega) = n^i(\omega)n^{i^*}(\omega) = \eta_3. \end{cases} \tag{33}$$

Rizzoli *et al.* [9] have computed the near-to-carrier phase noise

$$\ell(f_m) = \frac{1}{V^2\omega_m^2} \times \frac{\left(\frac{\partial G_T}{\partial V}\right)^2\eta_3 + \left(\frac{\partial B_T}{\partial V}\right)^2\eta_1 - 2\frac{\partial G_T}{\partial V}\frac{\partial B_T}{\partial V}{\rm Re}(\eta_2)}{\left(\frac{\partial G_T}{\partial \omega}\frac{\partial B_T}{\partial V} - \frac{\partial G_T}{\partial V}\frac{\partial B_T}{\partial \omega}\right)^2}. \tag{34}$$

Using the method described in this paper, we have calculated the same quantity, taking into account the noise cross correlation. The general relation for the phase noise is obtained by (30) using (13) and (14). Equation (35), shown at the bottom of the following page, describes off-the-carrier single-sideband noise. where α is given by (see Appendix B)

$$\alpha = 1 - \frac{1}{2V^3} \times \left[\frac{\left(\frac{\partial G_T}{\partial \omega}\right)^2\eta_1 + \left(\frac{\partial B_T}{\partial \omega}\right)^2\eta_3 + 2\frac{\partial G_T}{\partial \omega}\frac{\partial B_T}{\partial \omega}{\rm Re}(\eta_2)}{\left(\frac{\partial G_T}{\partial V}\frac{\partial B_T}{\partial \omega} - \frac{\partial G_T}{\partial \omega}\frac{\partial B_T}{\partial V}\right)\left(\left(\frac{\partial G_T}{\partial \omega}\right)^2 + \left(\frac{\partial B_T}{\partial \omega}\right)^2\right)} + \frac{\left(\frac{\partial G_T}{\partial V}\right)^2\eta_1 + \left(\frac{\partial B_T}{\partial V}\right)^2\eta_3 - 2\frac{\partial G_T}{\partial V}\frac{\partial B_T}{\partial V}{\rm Re}(\eta_2)}{\left(\frac{\partial G_T}{\partial V}\frac{\partial B_T}{\partial \omega} - \frac{\partial G_T}{\partial \omega}\frac{\partial B_T}{\partial V}\right)^3} \times \left(\left(\frac{\partial G_T}{\partial \omega}\right)^2 + \left(\frac{\partial B_T}{\partial \omega}\right)^2\right)\right]. \tag{36}$$

Relations obtained by Kurokawa [5] and Rizzoli *et al.* [9] are special cases of (35), namely, when $\eta_1 = \eta_3 = \eta$, $\eta_2 = 0$ and by neglecting the effect of amplitude fluctuations, (35) reduces to (32). When ω_m is very small and amplitude fluctutions are ignored, (35) reduces to (34).

$$\begin{cases} \ell_k(f_m) = \dfrac{P_{\rm Noise}(f-kf_0)}{P_{\rm carrier}} = \dfrac{1}{\alpha}\left[\dfrac{\big(\Delta V_{Lk}(\Omega_k)\big)\big(\Delta V_{Lk}(\Omega_k)\big)^*}{|V_{Lk}|^2} + \big(\Phi_{Lk}(\Omega_k)\big)\big(\Phi_{Lk}(\Omega_k)\big)^* + 2\,{\rm Im}\dfrac{\big(\Phi_{Lk}(\Omega_k)\big)\big(\Delta V_{Lk}(\Omega_k)\big)^*}{|V_{Lk}|}\right] \\ L_k(f_m) = 10\log_{10}(\ell_k(f_m)) \end{cases} \tag{30}$$

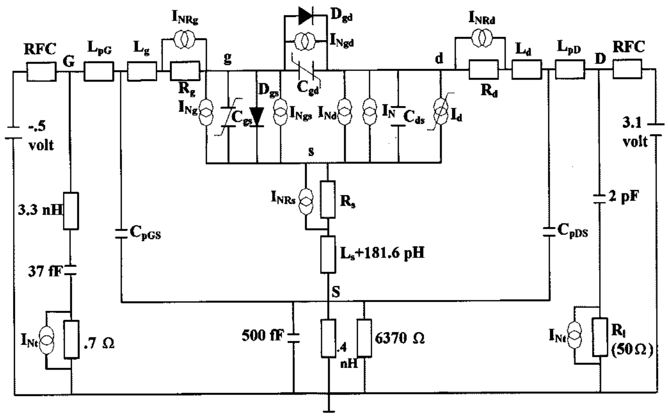

Fig. 4. NEC710 oscillator circuit diagram.

As such, the analytical relation presented here is a more precise version of the relations existing in the literature.

B. Noise Computation in an MESFET Oscillator

As another example, we have considered an MESFET oscillator, whose model is represented in Fig. 4. The single-sideband noise measurement of this oscillator has previously been made by Anzill *et al.* [10] with the given circuit details. We have developed our own nonlinear model for the NEC710 transistor and used the same noise sources with the same spectral distribution as used by Anzill. A total of nine noise sources have been considered. I_N, I_{Ng}, and I_{Nd} are nonwhite current noise sources.

Fig. 5 shows the single-sideband oscillator noise spectrum obtained by this harmonic-balance-based development along with the measurement points obtained by Anzill. White noise and $1/f$ noise contributions are shown separately. Reasonable accordance is observed up to 10 MHz off the carrier.

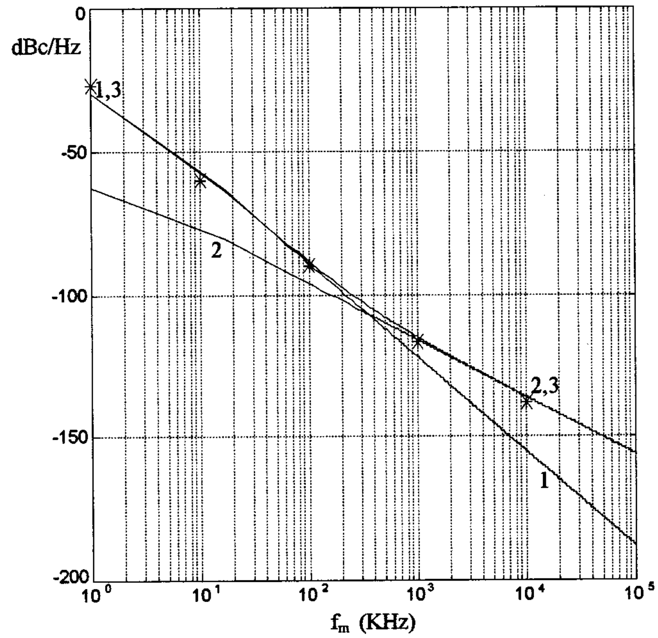

Fig. 5. Single-sideband noise spectrum of a 14.3-GHz MESFET oscillator. 1) $1/f$ noise contribution. 2) White-noise contribution. 3) Total spectrum. *: measured values [10].

VIII. Conclusion

In this paper, a unified treatment for the analysis of a microwave oscillator's spectrum was presented. Harmonic-balance resolution of the oscillator problem is the basis for this analysis. Matrix form derivatives of the harmonic-balance characteristic equation with respect to the harmonic amplitudes and frequency are used along with the noise vector spectral densities. A correlation matrix for the noise vector was defined, through which white or colored noise sources could be taken into account.

Amplitude and phase fluctuations in all ports and harmonics were calculated by matrix equations and from there on, the power spectrum of the voltages at any port were computed. Explicit relations for power spectral densities were obtained for any port voltage at any harmonic.

Analytical results of this treatment were compared to the existing litterature relations. Finally, the numerical results obtained for an MESFET oscillator were compared to the measurements made by Anzill *et al.*The method is general in the sense of circuit topology and noise source's distribution.

$$
\begin{aligned}
\ell(f_m) &= \Bigg[\frac{\left(\frac{\partial G_T}{\partial\omega}\right)^2\eta_3 + \left(\frac{\partial B_r}{\partial V}\right)^2\eta_1 - 2\frac{\partial G_T}{\partial\omega}\frac{\partial B_T}{\partial\omega}\mathrm{Re}(\eta_2)}{\alpha V^4\left(\frac{\partial G_T}{\partial V}\frac{\partial B_T}{\partial\omega} - \frac{\partial G_T}{\partial\omega}\frac{\partial B_T}{\partial V}\right)} \\
&+ \frac{\left(\left(\frac{\partial G_T}{\partial V}\right)^2 + \frac{\omega_m^2}{V^2}\left(\frac{\partial B_T}{\partial\omega}\right)^2\right)\eta_3 + \left(\left(\frac{\partial B_T}{\partial \mathbf{V}}\right)^2 + \frac{\omega_m^2}{V^2}\left(\frac{\partial G_T}{\partial\omega}\right)^2\right)\eta_1 - 2\,\mathrm{Re}(\eta_2)\left(\frac{\partial B_T}{\partial V}\frac{\partial G_T}{\partial V} - \frac{\omega_m^2}{V^2}\frac{\partial G_T}{\partial\omega}\frac{\partial B_T}{\partial\omega}\right)}{\alpha V^2\omega_m^2\left(\left(\frac{\partial G_T}{\partial V}\frac{\partial B_T}{\partial\omega} - \frac{\partial G_T}{\partial\omega}\frac{\partial B_T}{\partial V}\right)^2 + \frac{\omega_m^2}{V^2}\left(\left(\frac{\partial G_T}{\partial\omega}\right)^2 + \left(\frac{\partial B_T}{\partial\omega}\right)^2\right)^2\right)} \\
&+ \frac{\left(\frac{\partial B_T}{\partial V}\left(\frac{\partial B_T}{\partial\omega}\eta_1 - \frac{\partial G_T}{\partial\omega}\mathrm{Re}(\eta_2)\right)\right) + \left(\frac{\partial G_T}{\partial V}\left(\frac{\partial G_T}{\partial\omega}\eta_3 - \frac{\partial B_T}{\partial\omega}\mathrm{Re}(\eta_2)\right)\right) + \frac{\partial B_T}{\partial\omega}\frac{\partial G_T}{\partial\omega}\frac{\omega_m^2}{V^2}\left(\left(\frac{\partial G_T}{\partial\omega}\right)^2 + \left(\frac{\partial B_T}{\partial\omega}\right)^2\right)(\eta_3 - \eta_1)}{\frac{\alpha}{2}V^3\omega_m\left(\left(\frac{\partial G_T}{\partial V}\frac{\partial B_T}{\partial\omega} - \frac{\partial G_T}{\partial\omega}\frac{\partial B_T}{\partial V}\right)^2 + \frac{\omega_m^2}{V^2}\left(\left(\frac{\partial G_T}{\partial\omega}\right)^2 + \left(\frac{\partial B_T}{\partial\omega}\right)^2\right)^2\right)}\Bigg]
\end{aligned}
\tag{35}
$$

APPENDIX A

Here, we derive the exact expression for $R_{V_{m,k},V_{n,k}}(\tau)$ with phase-amplitude correlation and the corresponding simplified form for small phase and amplitude fluctuations.

Substituting $V_{m,k}$ and $V_{n,k}$ in (19), (A.1) is obtained as follows:

$$\begin{aligned} R_{v_{m,k},v_{n,k}}(\tau) &= \lim_{T\to\infty} \frac{1}{T} \int_{-\frac{T}{2}}^{\frac{T}{2}} \Big[\left(|V_{m,k}| + \Delta v_{m,k}(t)\right) \\ &\quad \times \cos\left(k\omega_0 t + \varphi_{0m,k} + \varphi_{m,k}(t)\right) \\ &\quad \times \left(|V_{n,k}| + \Delta v_{n,k}(t+\tau)\right) \\ &\quad \cdot \cos\left(k\omega_0 (t+\tau) + \varphi_{0n,k} + \varphi_{n,k}(t+\tau)\right)\Big]\, dt \end{aligned} \tag{A.1}$$

Using trigonometric rules and noting that the time variations of phase and amplitude fluctuations are much smaller than ω_0, (A.1) reduces to

$$\begin{aligned} R_{v_{m,k},v_{n,k}}(\tau) &= \lim_{T\to\infty} \frac{|V_{m,k}||V_{n,k}|}{2T} \int_{-\frac{T}{2}}^{\frac{T}{2}} \left(1 + \frac{\Delta v_{m,k}(t)}{|V_{m,k}|}\right) \\ &\quad \times \left(1 + \frac{\Delta v_{n,k}(t+\tau)}{|V_{n,k}|}\right) \\ &\quad \times \cos\left(k\omega_0 \tau - \varphi_{0m,k} + \varphi_{0n,k} - \varphi_{m,k}(t) + \varphi_{n,k}(t+\tau)\right) dt \end{aligned} \tag{A.2}$$

Equation (A.2) can be rewritten as

$$\begin{aligned} R_{v_{m,k},v_{n,k}}(\tau) &= \lim_{T\to\infty} \frac{|V_{m,k}||V_{n,k}|}{2T} \int_{-\frac{T}{2}}^{\frac{T}{2}} \left(1 + \frac{\Delta v_{m,k}(t)}{|V_{m,k}|}\right) \\ &\quad \times \left(1 + \frac{\Delta v_{n,k}(t+\tau)}{|V_{n,k}|}\right) \\ &\quad \times \Big[\cos(k\omega_0 \tau - \varphi_{0m,k} + \varphi_{0n,k}) \\ &\qquad \times \cos\left(\varphi_{m,k}(t) - \varphi_{n,k}(t+\tau)\right) \\ &\qquad + \sin(k\omega_0 \tau - \varphi_{0m,k} + \varphi_{0n,k}) \\ &\qquad \times \sin\left(\varphi_{m,k}(t) - \varphi_{n,k}(t+\tau)\right)\Big]\, dt. \end{aligned} \tag{A.3}$$

The above equation, which is the exact expression for $R_{V_{m,k},V_{n,k}}(\tau)$, can be written as (A.4) shown at the bottom of this page. By the fact that noise sources are small, the phase and amplitude fluctuations are small, thus, (A.4) can be approximated by

$$\begin{aligned} R_{v_{m,k},v_{n,k}}(\tau) &\approx \frac{|V_{m,k}||V_{n,k}|}{2} \Big[\cos(k\omega_0 \tau - \varphi_{0m,k} + \varphi_{0n,k}) \\ &\quad \times \Big[R_{(1-.5\varphi_{m,k}^2),(1-.5\varphi_{n,k}^2)} \\ &\quad + R_{\varphi_{m,k},\varphi_{n,k}} + R_{\frac{\Delta V_{m,k}}{|V_{m,k}|},\frac{\Delta V_{n,k}}{|V_{n,k}|}}\Big] \\ &\quad + \sin(k\omega_0 \tau - \varphi_{0m,k} + \varphi_{0n,k}) \\ &\quad \times \Big[R_{\varphi_{m,k},\frac{\Delta V_{n,k}}{|V_{n,k}|}} - R_{1,\frac{\Delta V_{n,k}}{|V_{n,k}|}\sin(\varphi_{n,k})} \\ &\quad + R_{\frac{\Delta V_{m,k}}{|V_{m,k}|}\sin(\varphi_{m,k}),1} - R_{\frac{\Delta V_{m,k}}{|V_{m,k}|},\varphi_{n,k}}\Big]\Big] \end{aligned} \tag{A.5}$$

where the third-order and higher order differentials are neglected. The former equation can be reduced to

$$\begin{aligned} R_{v_{m,k},v_{n,k}}(\tau) &= \frac{|V_{m,k}||V_{n,k}|}{2} \\ &\quad \cdot \Big[\cos(k\omega_0 \tau - \varphi_{0m,k} + \varphi_{0n,k}) \\ &\quad \times \Big[1 - .5\left(R_{\varphi_{m,k},\varphi_{m,k}}(0) + R_{\varphi_{n,k},\varphi_{n,k}}(0)\right) \\ &\quad + R_{\frac{\Delta v_{m,k}}{|V_{m,k}|},\frac{\Delta v_{n,k}}{|V_{n,k}|}}(\tau) + R_{\varphi_{m,k},\varphi_{n,k}}(\tau)\Big] \\ &\quad + \sin(k\omega_0 \tau - \varphi_{0m,k} + \varphi_{0n,k}) \\ &\quad \times \Big[R_{\varphi_{m,k},\frac{\Delta v_{n,k}}{|V_{n,k}|}}(\tau) - R_{\frac{\Delta v_{m,k}}{|V_{m,k}|},\varphi_{n,k}}(\tau) \\ &\quad + R_{\frac{\Delta v_{m,k}}{|V_{m,k}|},\varphi_{m,k}}(0) - R_{\varphi_{n,k},\frac{\Delta v_{n,k}}{|V_{n,k}|}}(0)\Big]\Big] \end{aligned} \tag{A.6}$$

which is exactly the same as (20).

$$\begin{aligned} R_{v_{m,k},v_{n,k}}(\tau) &= \frac{|V_{m,k}||V_{n,k}|}{2} \Big[\cos(k\omega_0 \tau - \varphi_{0m,k} + \varphi_{0n,k}) \\ &\quad \times \Big[R_{\cos(\varphi_{m,k}),\cos(\varphi_{n,k})} + R_{\sin(\varphi_{m,k}),\sin(\varphi_{n,k})} + R_{\cos(\varphi_{m,k}),\frac{\Delta V_{n,k}}{|V_{n,k}|}\cos(\varphi_{n,k})} + R_{\sin(\varphi_{m,k}),\frac{\Delta V_{n,k}}{|V_{n,k}|}\sin(\varphi_{n,k})} \\ &\quad + R_{\frac{\Delta V_{m,k}}{|V_{m,k}|}\cos(\varphi_{m,k}),\cos(\varphi_{n,k})} + R_{\frac{\Delta V_{m,k}}{|V_{m,k}|}\sin(\varphi_{m,k}),\sin(\varphi_{n,k})} + R_{\frac{\Delta V_{m,k}}{|V_{m,k}|}\cos(\varphi_{m,k}),\frac{\Delta V_{n,k}}{|V_{n,k}|}\cos(\varphi_{n,k})} \\ &\quad + R_{\frac{\Delta V_{m,k}}{|V_{m,k}|}\sin(\varphi_{m,k}),\frac{\Delta V_{n,k}}{|V_{n,k}|}\sin(\varphi_{n,k})}\Big] + \sin(k\omega_0 \tau - \varphi_{0m,k} + \varphi_{0n,k}) \\ &\quad \cdot \Big[R_{\sin(\varphi_{m,k}),\cos(\varphi_{n,k})} - R_{\cos(\varphi_{m,k}),\sin(\varphi_{n,k})} + R_{\sin(\varphi_{m,k}),\frac{\Delta V_{n,k}}{|V_{n,k}|}\cos(\varphi_{n,k})} - R_{\cos(\varphi_{m,k}),\frac{\Delta V_{n,k}}{|V_{n,k}|}\sin(\varphi_{n,k})} \\ &\quad + R_{\frac{\Delta V_{m,k}}{|V_{m,k}|}\sin(\varphi_{m,k}),\cos(\varphi_{n,k})} - R_{\frac{\Delta V_{m,k}}{|V_{m,k}|}\cos(\varphi_{m,k}),\sin(\varphi_{n,k})} + R_{\frac{\Delta V_{m,k}}{|V_{m,k}|}\sin(\varphi_{m,k}),\frac{\Delta V_{n,k}}{|V_{n,k}|}\cos(\varphi_{n,k})} \\ &\quad - R_{\frac{\Delta V_{m,k}}{|V_{m,k}|}\cos(\varphi_{m,k}),\frac{\Delta V_{n,k}}{|V_{n,k}|}\sin(\varphi_{n,k})}\Big]\Big] \end{aligned} \tag{A.4}$$

$$|\Phi(\omega)|^2 = \frac{\left(\left(\frac{\partial G_T}{\partial V}\right)^2 + \frac{\omega^2}{V^2}\left(\frac{\partial B_T}{\partial \omega}\right)^2\right)\eta_3 + \left(\left(\frac{\partial B_T}{\partial V}\right)^2 + \frac{\omega^2}{V^2}\left(\frac{\partial G_T}{\partial \omega}\right)^2\right)\eta_1 - 2\,\mathrm{Re}(\eta_2)\left(\frac{\partial B_T}{\partial V}\frac{\partial G_T}{\partial V} - \frac{\omega^2}{V^2}\frac{\partial G_T}{\partial \omega}\frac{\partial B_T}{\partial \omega}\right)}{\alpha V^2 \omega^2 \left(\left(\frac{\partial G_T}{\partial V}\frac{\partial B_T}{\partial \omega} - \frac{\partial G_T}{\partial \omega}\frac{\partial B_T}{\partial V}\right)^2 + \frac{\omega^2}{V^2}\left(\left(\frac{\partial G_T}{\partial \omega}\right)^2 + \left(\frac{\partial B_T}{\partial \omega}\right)^2\right)^2\right)} \qquad \text{(B.2)}$$

APPENDIX B

Here, the expressions for single-side-band noise in the Kurokawa oscillator are derived. Inserting the values of $\Delta V(\Omega)$, $\Phi(\Omega)$ from (13) and (14) into (30), where the harmonic-balance characteristic function $F(V, \omega_0)$ is replaced by (31a), taking into account the cross-correlation matrix of the in-phase and the quadrature components of the noise source, which is defined by (33), (35) is obtained.

In regard to definition of α, by substitution of (31a) into (26), taking into account the expression (33), one gets (B.2), shown at the top of this page.

$$\alpha = 1 - \frac{1}{2\pi}\int_{-\infty}^{\infty} \left(\Phi(\omega)\right)\left(\Phi(\omega)\right)^* d\omega. \qquad \text{(B.1)}$$

By insertion of (B.2) in (B.1) and integrating, one obtains α as

$$\alpha = 1 - \frac{1}{2V^3} \times \left[\frac{\left(\frac{\partial G_T}{\partial \omega}\right)^2 \eta_1 + \left(\frac{\partial B_T}{\partial \omega}\right)^2 \eta_3 + 2\frac{\partial G_T}{\partial \omega}\frac{\partial B_T}{\partial \omega}\mathrm{Re}(\eta_2)}{\left(\frac{\partial G_T}{\partial V}\frac{\partial B_T}{\partial \omega} - \frac{\partial G_T}{\partial \omega}\frac{\partial B_T}{\partial V}\right)\left(\left(\frac{\partial G_T}{\partial \omega}\right)^2 + \left(\frac{\partial B_T}{\partial \omega}\right)^2\right)} + \frac{\left(\frac{\partial G_T}{\partial V}\right)^2 \eta_1 + \left(\frac{\partial B_T}{\partial \omega}\right)^2 \eta_3 - 2\frac{\partial G_T}{\partial V}\frac{\partial B_T}{\partial V}\mathrm{Re}(\eta_2)}{\left(\frac{\partial G_T}{\partial V}\frac{\partial B_T}{\partial \omega} - \frac{\partial G_T}{\partial \omega}\frac{\partial B_T}{\partial V}\right)^3} \times \left(\left(\frac{\partial G_T}{\partial \omega}\right)^2 + \left(\frac{\partial B_T}{\partial \omega}\right)^2\right)\right]. \qquad \text{(B.3)}$$

REFERENCES

[1] R. A. Pucel and J. Curtis, "Near carrier noise in FET oscillators," in *IEEE MTT-S Int. Microwave Symp. Dig.*, 1983, pp. 282–284.

[2] B. T. Debney and J. S. Joshi, "A theory of noise in GaAs FET microwave oscillators and its experimental verification," *IEEE Trans. Electron Devices*, vol. ED-30, pp. 769–776, July 1983.

[3] A. N. Riddle and R. J. Trew, "A novel GaAs FET oscillator with low phase noise," in *IEEE MTT-S Int. Microwave Symp. Dig.*, 1985, pp. 257–260.

[4] J. Verdier, O. Llopis, R. Plana, and J. Graffeuil, "Analysis of noise up-conversion in microwave field-effect transistor oscillators," *IEEE Trans. Microwave Theory Tech.*, vol. 44, pp. 1478–1483, Aug. 1996.

[5] K. Kurokawa, "Noise in synchronized oscillators," *IEEE Trans. Microwave Theory Tech.*, vol. MTT-16, pp. 234–240, Apr. 1968.

[6] M. Prigent, J. C. Nallatamby, E. Ngoya, R. Quere, and J. Obregon, "Simulation techniques of nonlinear circuit dynamic behavior," *Ann. Telecommun.*, vol. 51, no. 9–10, pp. 541–552, 1996.

[7] J. M. Paillot *et al.*, "A general program for steady state stability and FM noise analysis of microwave oscillators," in *IEEE MTT-S Int. Microwave Symp. Dig.*, 1990, pp. 1287–1290.

[8] H. J. Siweris and B. Schieck, "Analysis of noise up conversion in microwave FET oscillators," *IEEE Trans. Microwave Theory Tech.*, vol. MTT-33, pp. 233–242, Mar. 1985.

[9] V. Rizzoli, F. Masteri, and D. Masotti, "General noise analysis of nonlinear microwave circuits by piecewise harmonic-balance technique," *IEEE Trans. Microwave Theory Tech.*, vol. 42, pp. 807–819, May 1994.

[10] W. Anzill, M. Fillebock, and P. Russer, "Low phase noise design of microwave oscillators," *Int. J. Microwave Millimeter-Wave Computer-Aided Eng.*, vol. 6, no. 1, pp. 5–25, 1996.

[11] F. Farzaneh and E. Mehrshahi, "A new quasi-Newton method in harmonic balance analysis of microwave oscillator," *Rev. High-Frequency Tijdschrift*, vol. XXI, no. 4, pp. 55–62, Dec. 1997.

[12] R. J. Gilmore and M. B. Steer, "Nonlinear circuit analysis using the method of harmonic balance—A review of the art. part 1. Introductory concepts," *Int. J. Microwave Millimeter-Wave Computer-Aided Eng.*, vol. 1, pp. 22–37, Jan. 1991.

[13] F. Farzaneh and E. Mehrshahi, "A novel noise analysis method in microwave oscillators based on harmonic balance," in *Proc. 28th European Microwave Conf.*, Amsterdam, The Netherlands, Oct. 5–9, 1998, pp. 256–260.

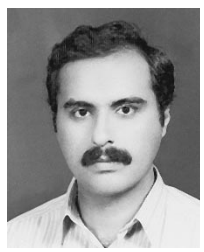

Esfandiar Mehrshahi was born in Tehran, Iran, in 1963. He received the B.Sc. degree from the Iran University of Science and Technology, Tehran, Iran, in 1987, and the M.Sc. and Ph.D. degrees from the Sharif University of Technology, Tehran, Iran, in 1991 and 1998, respectively.

Since 1990, he has been involved in several research and engineering projects at the Iran Telecommunications Research Center (ITRC). He is currently an Assistant Professor at Shahid Beheshti University, Tehran, Iran. His main areas of interest are the nonlinear simulation of microwave circuits and microwave oscillator's spectrum.

Forouhar Farzaneh (S'82–M'84–SM'96) was born in Tehran, Iran, in 1957. He received the B.Sc. degree in electrical engineering from Shiraz University, Shiraz, Iran, in 1980, the CES degree in telecommunications from ENST-Paris, Paris, France, in 1981, and the DEA and Docteur Ingenieur degrees from the University of Limoges, Limoges, France, in 1982 and 1985, respectively.

From 1985 to 1989, he was with the Tehran Polytechnic University, as a faculty member. Since 1989, he has been with the Sharif University of Technology, Tehran, Iran, where he is an Associate Professor of electrical engineering. Since 1989, he has been involved in several research and engineering projects in the field of microwaves and radio communications. During the 1996–1997 academic year, he was with the Microwave Laboratory, Université Catholique de Louvain, Louvain, Belgium, as a Visiting Professor. Since 1996, he has been nominated as a member of the Higher Education Board in Electrical Engineering, Ministry of Culture and Higher Education, Iran. His main areas of interest are the nonlinear simulation of microwave circuits and link analysis in microwave/satellite radiocommunications.

Dr. Farzaneh was a co-recipient of the 1985 European Microwave Prize.